

Lithium copper/manganese titanate anode material for rechargeable lithium-ion batteries



Wei Chen ^a, Zhengrong Zhou ^a, Hanfeng Liang ^a, Weijian Ren ^c, Jie Shu ^{b, **},
Zhoucheng Wang ^{a, *}

^a College of Chemistry and Chemical Engineering, Xiamen University, Xiamen 361005, China

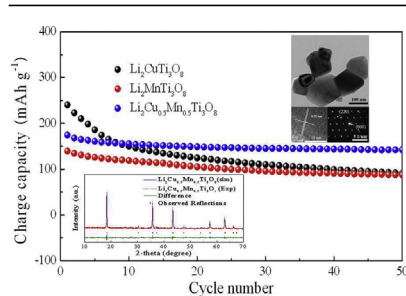
^b Faculty of Materials Science and Chemical Engineering, Ningbo University, Ningbo 315211, China

^c College of Materials, Xiamen University, Xiamen 361005, China

HIGHLIGHTS

- Spinel $\text{Li}_2\text{Cu}_{0.5}\text{Mn}_{0.5}\text{Ti}_3\text{O}_8$ is prepared by a simple solid state reaction.
- $\text{Li}_2\text{Cu}_{0.5}\text{Mn}_{0.5}\text{Ti}_3\text{O}_8$ shows better electrochemical property than $\text{Li}_2\text{CuTi}_3\text{O}_8$ and $\text{Li}_2\text{MnTi}_3\text{O}_8$.
- $\text{Li}_2\text{Cu}_{0.5}\text{Mn}_{0.5}\text{Ti}_3\text{O}_8$ reveals a reversible capacity of 143 mAh g^{-1} after 50 cycles.

GRAPHICAL ABSTRACT



ARTICLE INFO

Article history:

Received 17 December 2014

Received in revised form

30 March 2015

Accepted 21 November 2015

Available online 28 November 2015

Keywords:

Electronic materials

Sintering

Electron microscopy

Crystal structure

Electrochemical properties

ABSTRACT

In this article, Cu^{2+} and Mn^{2+} are chosen as divalent metal cations to dope and synthesize $\text{Li}_2\text{MTi}_3\text{O}_8$ ($\text{M} = \text{Cu}, \text{Mn}, \text{Cu}_{0.5}\text{Mn}_{0.5}$) by a simple solid state reaction route. The structures of $\text{Li}_2\text{MTi}_3\text{O}_8$ ($\text{M} = \text{Cu}, \text{Mn}, \text{Cu}_{0.5}\text{Mn}_{0.5}$) are proved by Rietveld refinement method for the first time. Due to different divalent metal cations M^{2+} in the structure, $\text{Li}_2\text{MTi}_3\text{O}_8$ exhibits different electrochemical performances. $\text{Li}_2\text{CuTi}_3\text{O}_8$ shows the highest initial charge capacity of 242 mAh g^{-1} and $\text{Li}_2\text{MnTi}_3\text{O}_8$ displays the lowest initial charge capacity of 139.5 mAh g^{-1} among all the three samples. Although $\text{Li}_2\text{Cu}_{0.5}\text{Mn}_{0.5}\text{Ti}_3\text{O}_8$ reveals a lower initial charge capacity of 174.5 mAh g^{-1} , it exhibits better cycle performance than $\text{Li}_2\text{CuTi}_3\text{O}_8$ and $\text{Li}_2\text{MnTi}_3\text{O}_8$. $\text{Li}_2\text{Cu}_{0.5}\text{Mn}_{0.5}\text{Ti}_3\text{O}_8$ keeps the reversible capacity of 143 mAh g^{-1} after 50 cycles at 100 mA g^{-1} with capacity retention of 82.2%. Besides, the results of electrochemical impedance spectra indicate that lithium ion can move easily in the tunnels of three-dimensional network formed by the $(\text{Li}_{0.7}\text{Cu}_{0.15}\text{Mn}_{0.25})^{\text{tet}}$, which is in agreement with the result that $\text{Li}_2\text{Cu}_{0.5}\text{Mn}_{0.5}\text{Ti}_3\text{O}_8$ performs better electrochemical properties than $\text{Li}_2\text{CuTi}_3\text{O}_8$ and $\text{Li}_2\text{MnTi}_3\text{O}_8$. It provides a possibility and theoretical support to synthesize Ti-based materials $\text{Li}_2\text{MTi}_3\text{O}_8$ with good electrochemical performances.

© 2015 Elsevier B.V. All rights reserved.

1. Introduction

In recent years, the research and development of hybrid electric vehicle, plug-in hybrid electric and electric vehicle have been intensified due to the energy crisis and environmental concerns

* Corresponding author.

** Corresponding author.

E-mail addresses: sergio_shu@hotmail.com (J. Shu), zcwang@xmu.edu.cn (Z. Wang).

[1–4]. Compared to other energy storage devices, lithium ion batteries (LIBs) dominate as the main power source for portable electronic devices. The commonly used graphite anode in LIBs exhibits an excellent cycling behavior, but the main drawback is electrolyte reduction during Li intercalation into graphitic layers, which causes the formation of a solid–electrolyte interface layer (SEI), which also decreases the life span of a battery. Additionally, metallic Li will be deposited on the electrode at high current densities which may lead to serious safety problem. Therefore, researchers must identify a suitable material for the anodes working at a higher potential than the currently used carbon or graphite electrodes (-1 V versus lithium) which are to be replaced for safety reasons [1,2].

Titanium oxides with the $\text{Ti}^{4+}/\text{Ti}^{3+}$ redox couple working at approximately 1.5 V versus lithium fulfill this requirement [5–17]. More recently, $\text{Li}_2\text{MTi}_3\text{O}_8$ ($M = \text{Co}, \text{Zn}, \text{Mg}$) have been synthesized and exhibited excellent electrochemical performances [8,9]. Based on previous reports, electrochemical measurements indicated that $\text{Li}_2\text{CoTi}_3\text{O}_8$ fibers delivered a specific capacity of 388 mAh g^{-1} for the first cycle and the reversible capacity retained at 237 mAh g^{-1} after 30 cycles with a current density of 50 mA g^{-1} [14]. Besides, $\text{Li}_2\text{ZnTi}_3\text{O}_8$ nanowires revealed a good electrochemical reversibility between 0.2 and 3.0 V with reversible capacities of 219.9 mAh g^{-1} and 150 mAh g^{-1} at current densities of 30 mA g^{-1} and 240 mA g^{-1} , respectively [11]. However, the disadvantage of $\text{Li}_2\text{MTi}_3\text{O}_8$ is its poor electronic conductivity and lithium ion diffusion coefficient that limits its full capacity at high charge–discharge rates. At high charge and discharge rates, high Li^+ ion insertion and exertion flux on the electrode surface and slow Li^+ ion transport result in concentration polarization of Li^+ ion within the electrode material. This phenomenon causes a drop of the cell voltage, which results in termination of the discharge before the electrode material reaching the maximum capacity. Based on these previous reports, it is obvious that most of these works focused on investigating the electrochemical properties by using nanostructure materials and ignored optimizing this kind of material by doping as a matter of fact.

Inspired by these studies, $\text{Li}_2\text{CuTi}_3\text{O}_8$, $\text{Li}_2\text{MnTi}_3\text{O}_8$ and $\text{Li}_2\text{Cu}_{0.5}\text{Mn}_{0.5}\text{Ti}_3\text{O}_8$ were synthesized successfully by a solid–state reaction route and their comparative lithium storage properties were also investigated. And the result shows that the $\text{Li}_2\text{Cu}_{0.5}\text{Mn}_{0.5}\text{Ti}_3\text{O}_8$ exhibited better electrochemical performance compared to other two materials.

2. Experimental

2.1. Preparation of materials

All the spinels $\text{Li}_2\text{MTi}_3\text{O}_8$ ($M = \text{Cu}, \text{Mn}, \text{Cu}_{0.5}\text{Mn}_{0.5}$) were synthesized by a solid–state reaction as follows. Stoichiometric amounts of lithium carbonate (Li_2CO_3), nano-size titanium dioxide (TiO_2), manganese acetate tetrahydrate ($\text{Mn}(\text{CH}_3\text{COO})_2 \cdot 4\text{H}_2\text{O}$) and/or cupric acetate hydrate ($\text{Cu}(\text{CH}_3\text{COO})_2 \cdot \text{H}_2\text{O}$) were ground by mechanical ball-milling in the agate jar at 400 rpm for 12 h. The as-obtained powdery mixture was calcined at 750°C for 5 h and then cooled down to room temperature naturally. As a result, $\text{Li}_2\text{MTi}_3\text{O}_8$ ($M = \text{Cu}, \text{Mn}, \text{Cu}_{0.5}\text{Mn}_{0.5}$) were synthesized successfully.

2.2. Characterization of materials

The as-prepared products were characterized by X-ray powder diffraction (XRD) on a Rigaku Ultima IV XRD. The wavelengths of the X-rays are $K\alpha_1 = 1.5406$ and $K\alpha_2 = 1.54439$, respectively. The data of the samples were collected by a step of 0.02° at the scanning speed of $30^\circ \text{ min}^{-1}$ over the 2θ range of 10 – 70° at room

temperature. The differences in structures for different $\text{Li}_2\text{MTi}_3\text{O}_8$ ($M = \text{Cu}, \text{Mn}$ or $\text{Cu}_{0.5}\text{Mn}_{0.5}$) were checked by XRD Rietveld refinement. Here, the program FullProf was used for crystal structure refinements, employing the Rietveld method. Scanning electron microscopy (SEM) images and energy dispersive spectrometer (EDS) measurements were recorded on a LEO 1530 microscope (Germany). Transmission electron microscopy (TEM) pictures, high-resolution TEM (HRTEM) images and the corresponding selected area electron diffraction (SAED) patterns were performed using a JEOL JEM-2100 transmission electron microscope at an accelerating voltage of 200 kV.

2.3. Electrode fabrication and electrochemical test

The electrochemical properties of $\text{Li}_2\text{MTi}_3\text{O}_8$ ($M = \text{Cu}, \text{Mn}, \text{Cu}_{0.5}\text{Mn}_{0.5}$) were evaluated by two-electrode system in which metallic lithium was used as the counter electrode. The working electrode was prepared by the following steps. Active material, acetylene black and polyvinylidene fluoride at a weight ratio of 8:1:1 were dispersed in *N*-methyl-pyrrolidinone. The mixed slurry was spread on a Cu foil substrate to form a thin film after being ground vigorously. Then the film was dried in a vacuum oven at 120°C for 24 h. The cells were charged and discharged in the potential range of 0.0–3.0 V (vs. Li^+/Li) at the current density of 100 mA g^{-1} . In addition, electrochemical impedance spectroscopy (EIS) patterns were recorded on a CHI660 electrochemical workstation in the frequency range from 0.01 to 100,000 Hz.

3. Results and discussion

The XRD patterns and corresponding Rietveld refinement plots of as-synthesized $\text{Li}_2\text{MTi}_3\text{O}_8$ ($M = \text{Cu}, \text{Mn}, \text{Cu}_{0.5}\text{Mn}_{0.5}$) powders are shown in Fig. 1a, b and c. The atomic sites of $\text{Li}_2\text{CuTi}_3\text{O}_8$, $\text{Li}_2\text{MnTi}_3\text{O}_8$, $\text{Li}_2\text{Cu}_{0.5}\text{Mn}_{0.5}\text{Ti}_3\text{O}_8$ and corresponding refinement character factors are shown in Table 1. It is clear that $\text{Li}_2\text{CuTi}_3\text{O}_8$ can be described as $(\text{Li}_{0.7}\text{Cu}_{0.3})^{\text{tet}}[\text{Li}_{0.3}\text{Cu}_{0.2}\text{Ti}_{1.5}]^{\text{oct}}\text{O}_4$ (Fig. 2a), $\text{Li}_2\text{MnTi}_3\text{O}_8$ as $(\text{Li}_{0.505}\text{Mn}_{0.495})^{\text{tet}}(\text{Li}_{0.495}\text{Mn}_{0.005})^{\text{oct}}\text{Ti}_{1.5}^{\text{oct}}\text{O}_4$ (Fig. 2b) and $\text{Li}_2\text{Cu}_{0.5}\text{Mn}_{0.5}\text{Ti}_3\text{O}_8$ as $(\text{Li}_{0.7}\text{Cu}_{0.15}\text{Mn}_{0.25})^{\text{tet}}[\text{Li}_{0.3}\text{Cu}_{0.1}\text{Ti}_{1.5}]^{\text{oct}}\text{O}_4$ (Fig. 2c). The unit cell parameters have been worked out by Rietveld refinement. The values of $\text{Li}_2\text{MTi}_3\text{O}_8$ ($M = \text{Cu}, \text{Mn}, \text{Cu}_{0.5}\text{Mn}_{0.5}$) are 8.3581, 8.3881 and 8.3458 Å, respectively. The profile R value (R_p), weighted-profile R value (R_{wp}) and χ^2 value of the refined structure parameters indicate that the refinement result are acceptable.

For $\text{Li}_2\text{CuTi}_3\text{O}_8$ (Fig. 1a), the XRD pattern can be indexed to a cubic structure of space group of Fd-3m (JCPDS card No. 49–0448). In this structure of $(\text{Li}_{0.7}\text{Cu}_{0.3})^{\text{tet}}[\text{Li}_{0.3}\text{Cu}_{0.2}\text{Ti}_{1.5}]^{\text{oct}}\text{O}_4$, the octahedron which is constituted by Li, Cu and Ti atoms provides a stable frame during lithiation and de-lithiation process. This is the reason that Ti-based material has excellent cycling performance. The $\text{Li}_2\text{CuTi}_3\text{O}_8$ is built on two sets of octahedrons of TiO_6 and $\text{Li}(\text{Cu})\text{O}_6$. Thus, a three-dimensional network is formed in such a structure, where Li(Cu) atoms are located in tetrahedral sites forming tunnels [13]. In contrast, $\text{Li}_2\text{MnTi}_3\text{O}_8$ is confirmed as a cubic structure of space group of P4₃32 by XRD pattern. The structure of $\text{Li}_2\text{MnTi}_3\text{O}_8$ (Fig. 2b) is also composed of octahedrons and tetrahedrons like $\text{Li}_2\text{CuTi}_3\text{O}_8$. Different from $\text{Li}_2\text{CuTi}_3\text{O}_8$, the frame of $\text{Li}_2\text{MnTi}_3\text{O}_8$ is formed by octahedrons located by Ti atoms and octahedrons located by a part of Li and Mn atoms. The atomic radius of Mn (140 pm) is bigger than Cu (135 pm) leading to a compressed unit cell, which makes the octahedrons of $\text{Li}_2\text{MnTi}_3\text{O}_8$ become thinner than those of $\text{Li}_2\text{CuTi}_3\text{O}_8$ (Fig. 2b). Due to the similar XRD patterns between $\text{Li}_2\text{Cu}_{0.5}\text{Mn}_{0.5}\text{Ti}_3\text{O}_8$ and $\text{Li}_2\text{CuTi}_3\text{O}_8$, the structure of $\text{Li}_2\text{Cu}_{0.5}\text{Mn}_{0.5}\text{Ti}_3\text{O}_8$ can be described as $(\text{Li}_{0.7}\text{Cu}_{0.15}\text{Mn}_{0.25})^{\text{tet}}[\text{Li}_{0.3}\text{Cu}_{0.1}\text{Ti}_{1.5}]^{\text{oct}}\text{O}_4$ close to $\text{Li}_2\text{CuTi}_3\text{O}_8$. The decrease of relative intensities of main diffraction peaks are detected for

Download English Version:

<https://daneshyari.com/en/article/1521037>

Download Persian Version:

<https://daneshyari.com/article/1521037>

[Daneshyari.com](https://daneshyari.com)